International Journal of Heat and Mass Transfer 202 (2023) 123723

Contents lists available at ScienceDirect

International Journal of Heat and Mass Transfer

journal homepage: www.elsevier.com/locate/hmt

Theoretical analysis of a two-dimensional multilayer diffusion problem with general convective boundary conditions normal to the layered direction

Girish Krishnan, Ankur Jain*

Mechanical and Aerospace Engineering Department, University of Texas at Arlington, 500 W First St, Rm 211, Arlington, TX, USA

ARTICLE INFO

Article history:
Received 23 August 2022
Revised 5 November 2022
Accepted 26 November 2022

Keywords:
Multilayer thermal conduction
Laplace transforms
Convective boundary conditions
Analytical modeling

ABSTRACT

Theoretical analysis of transient thermal conduction in a two-dimensional multilayer structure has been limited to problems with isothermal or adiabatic boundary conditions along the walls normal to the layered direction. Due to mathematical difficulties pointed out in past work, an analytical solution has not been possible so far for the general case where each layer has a distinct convective boundary condition. This work presents an analytical technique to solve this general problem using Laplace transforms followed by derivation of a sufficient number of linear algebraic equations based on given boundary conditions to determine the coefficients of an eigenfunction-based series solution. This technique makes it possible to solve the problem when each layer may have a different convective heat transfer coefficient along the walls normal to the layered direction. Results from this general analysis are shown to correctly reduce to past work for the special cases of very small or very large Biot number. Good agreement with specific results presented in a past paper is also demonstrated. The technique is used to investigate the impact of key dimensionless parameters on the temperature field. This work significantly generalizes past work that was limited only to adiabatic or isothermal boundary conditions. Results presented here may help improve the theoretical understanding of multilayer diffusion problems, and make theoretical models much more representative of realistic conditions.

1. Introduction

Heat and mass transfer in a multilayer body is of much interest in a broad variety of engineering processes. For example, heat transfer in multilayer Li-ion cells ultimately determines the safety and efficiency of the cells [1]. Multilayer heat transfer also occurs in semiconductor devices/systems [2], atmospheric re-entry [3], extended surfaces [4] and nuclear engineering [5]. In addition, multilayer mass transport is also relevant in problems related to ionic transport in Li-ion cells [6,7] and drug delivery [8].

The theoretical modeling of one-dimensional multilayer diffusion is quite well developed. While complex variables [9] and the adjoint method [10] have been used for this purpose, the most common technique is separation of variables with quasi-orthogonal eigenfunctions [11]. In this technique, an infinite series solution is written for each layer, and a single set of eigenvalues is derived by accounting for all boundary and interface conditions. Quasi-orthogonality of eigenfunctions is utilized for deriving the coefficients that appear in the series solution [12]. Multilayer problems with more complicated features, such as spatially-dependent [13] or time-dependent [14] boundary conditions, convective transport [15], reaction [16], multispecies advection-dispersion [17] and a large number of layers [18] have also been analyzed in the past. Imaginary eigenvalues are known to appear in a subset of such problems, which have been related to divergence of the temperature field at large times [15,16,19].

While one-dimensional analysis is sufficient for a large number of engineering problems, in some cases, a two- or three-dimensional analysis is necessitated. Such problems have been analyzed in both steady-state [20] and transient conditions [21–24]. Fig. 1 presents a general schematic of this problem both for an *M*-layer body and the special case of a two-layer body. Steady-state analysis of a two-dimensional multilayer body is, in principle, similar to transient analysis of a one-dimensional multilayer body [11]. However, transient analysis of two-dimensional multilayer problems is a lot more complicated, particularly with general boundary conditions.

Past literature on multilayer two- or three-dimensional problems is limited to cases where boundary conditions along the walls normal to the layered direction are either isothermal or adiabatic

* Corresponding author.
E-mail address: jaina@uta.edu (A. Jain).

https://doi.org/10.1016/j.ijheatmasstransfer.2022.123723
0017-9310/

Nomenclature

Bi	Biot number, $Bi = \frac{hx_M}{k_M}$
h	convective heat transfer coefficient ($Wm^{-2}K^{-1}$)
k	thermal conductivity ($Wm^{-1}K^{-1}$)
$\bar{k}$	non-dimensional thermal conductivity, $\bar{k}_m = \frac{k_m}{k_M}$
M	number of layers
s	Laplace variable
T	temperature (K)
t	time (s)
w	half-width of the body in the y direction (m)
$\bar{w}$	non-dimensional half-width of the body in the y direction, $\bar{w} = \frac{w}{x_M}$
x, y	spatial coordinates (m)
α	diffusivity (m^2s^{-1})
$\bar{\alpha}$	non-dimensional diffusivity, $\bar{\alpha}_m = \frac{\alpha_m}{\alpha_M}$
η, ξ	non-dimensional spatial coordinates, $\eta = \frac{y}{x_M}$; $\xi = \frac{x}{x_M}$
γ	non-dimensional interface location, $\gamma_m = \frac{x_m}{x_M}$
τ	non-dimensional time, $\tau = \frac{\alpha_M t}{x_M^2}$
θ	non-dimensional temperature, $\theta_m = \frac{T_m - T_{amb}}{T_{ref} - T_{amb}}$
$\hat{\theta}$	Laplacian of the temperature field
λ	non-dimensional eigenvalue in η direction

Subscripts

A	x=0 boundary
amb	ambient
B	x=x_M boundary
in	initial temperature
m	layer number
ref	reference

[21–24]. For these special cases, it is possible to derive an infinite series solution with the same set of eigenvalues for each layer, which can easily satisfy interface conditions. In addition to such separation of variables based techniques, a technique that uses Laplace transforms has also been used to analyze such problems with isothermal or adiabatic boundary conditions [25–27]. However, the more general case of convective boundary conditions in the direction normal to the layers presents considerable mathematical difficulty and has explicitly not been solved in past work [21–24]. For example, past work on transient two-dimensional multilayer analysis [21,22] has clearly excluded the case where this boundary condition is not isothermal or adiabatic. When each layer has unique thermal properties and convective heat transfer coefficients, such as shown in Fig. 1(a), the separation of variables technique results in a unique set of eigenvalues for each layer, which presents an "unconditional mathematical difficulty" [22] by making it difficult to satisfy interface conditions. This difficulty does not arise in the special cases of isothermal or adiabatic boundary conditions (i.e., $Bi \to \infty$ or $Bi = 0$, respectively), for which, solutions are readily available [21–24].

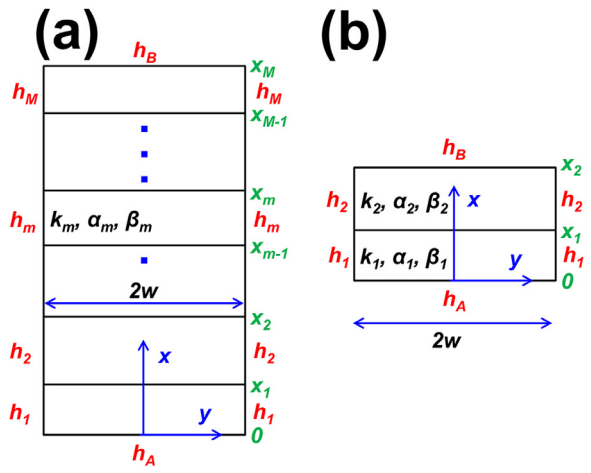

Fig. 1. Schematic of the two-dimensional multilayer diffusion-reaction problem considered here: (a) The general M-layer problem, and (b) specific two-layer problem (M=2). In both cases, each layer has distinct convective heat transfer coefficient h_m (m=1,2..M) along the walls normal to the layered direction.

It is desirable to extend theoretical analysis of thermal conduction in a two-dimensional multilayer geometry to include general convective boundary conditions on the walls normal to the layered direction. Despite the difficulties presented by the general convective case, as outlined above, such analysis will be more representative of realistic scenarios, where a convective coefficient is more appropriate than the extreme isothermal or adiabatic conditions. Moreover, doing so may advance the state-of-the-art in multilayer diffusion/reaction analysis by overcoming a known theoretical difficulty, as acknowledged by past work [21,22]. One possible technique to solve this general problem is to consider a finite number of terms in the series solution and then derive a sufficient number of linear algebraic equations to determine the unknown but finite number of coefficients. This technique has been used in the past for solving problems related to thermal conduction in fins [28], cylinders [29] and multilayer structures [13,30]. In addition, a similar technique has recently been used to solve a 2D steady-state diffusion problem in a locally-isotropic heterogeneous body [31]. Even though considering a finite number of terms in the series solution involves an approximation, doing so is no worse than practical computation of the infinite series solution, for which also, only a finite number of terms can be practically considered.

This work analyzes a transient two-dimensional multilayer diffusion problem with general convective boundary conditions along the surfaces normal to the layered direction. A Laplace transform is first carried out, followed by a variable transformation. A series solution for the resulting problem is written using the separation of variables technique. Finally, a sufficient set of algebraic equations is derived for determining the coefficients that appear in the series solution. By doing so, an explicit solution for the problem is derived, despite unequal thermal properties and general convective coefficients in each layer. This represents a significant generalization of past results that were limited only to adiabatic or isothermal conditions. Results from the present work are shown to correctly reduce to past results for various special cases. The generalization to convective conditions offered by the present technique helps improve the theoretical understanding of multilayer diffusion, and makes theoretical models much more representative of realistic conditions.

Section 2 defines the problem addressed in this work, as well as non-dimensionalization scheme. Results for the general two-dimensional M-layer case are presented in Section 3, followed by the special case of a two-layer body. A discussion of key results, including verification of results and comparison with past work is presented in Section 4.

2. Mathematical modeling

2.1. Problem definition for general M-layer case

Consider the transient diffusion problem in a two-dimensional M-layer body of width $2w$ and thicknesses $x_m - x_{m-1}$ for each layer, m=1,2..M, as shown in Fig. 1(a). Isotropic thermal conductivity and diffusivity of each layer is k_m and α_m, respectively. Ad-

jacent layers are assumed to be in perfect thermal contact with each other. All properties are assumed to be independent of temperature. The top and bottom boundaries of the geometry are characterized with convective heat transfer coefficients h_A and h_B, respectively, as shown in Fig. 1(a). Both side walls of each layer are characterized by a general convective heat transfer coefficient h_m, m=1,2..M. Each layer in the body is at an initial non-zero and uniform temperature $T_{in,m}$, and the interest is in determining the evolution of the temperature distribution in each layer as a function of time.

The problem defined here is a generalization of past papers on thermal conduction in two-dimensional multilayer bodies. For example, both Haji-Sheikh & Beck [21] and de Monte [22] considered only isothermal and adiabatic boundary conditions on the side walls. In contrast, the present work accounts for the more general convective boundary condition that was explicitly excluded in such past work. Moreover, while such papers were limited to a two-layer body, the present work generalizes the treatment to an arbitrary number of layers.

Since the problem is symmetric about the center line of the geometry, it is possible to consider only one half of the problem. In such a case, the governing energy equation for the temperature field $T_m(x, y, t)$ in the right half of the geometry is

$$\alpha_m\left(\frac{\partial^2 T_m}{\partial x^2}+\frac{\partial^2 T_m}{\partial y^2}\right)=\frac{\partial T_m}{\partial t}(m=1,2..M) \tag{1}$$

subject to boundary conditions given by

$$-k_1\frac{\partial T_1}{\partial x}+h_A(T_1-T_{amb})=0 \quad (x=0) \tag{2}$$

$$k_M\frac{\partial T_M}{\partial x}+h_B(T_M-T_{amb})=0 \quad (x=x_M) \tag{3}$$

$$\frac{\partial T_m}{\partial y}=0 \quad (y=0) \tag{4}$$

$$k_m\frac{\partial T_m}{\partial y}+h_m(T_m-T_{amb})=0 \quad (y=w) \tag{5}$$

In addition, based on interfacial energy conservation and temperature continuity, the following interface conditions apply for m=1,2..M-1.

$$T_m=T_{m+1} \quad (x=x_m) \tag{6}$$

$$k_m\frac{\partial T_m}{\partial x}=k_{m+1}\frac{\partial T_{m+1}}{\partial x} \quad (x=x_m) \tag{7}$$

A uniform initial temperature is assumed in each layer, i.e.,

$$T_m=T_{m,in} \quad (t=0)(m=1,2..M) \tag{8}$$

2.2. Non-dimensionalization

Before solving this problem with general convective boundary conditions along the boundary normal to the layered direction ($y=w$) given by Eq. (5), a non-dimensionalization is first carried out based on the following:

$$\begin{aligned}&\theta_m=\tfrac{T_m-T_{amb}}{T_{ref}-T_{amb}},\ \xi=\tfrac{x}{x_M},\ \eta=\tfrac{y}{x_M},\ \tau=\tfrac{\alpha_M t}{x_M^2},\ \gamma_m=\tfrac{x_m}{x_M},\\ &\bar{w}=\tfrac{w}{x_M},\ \bar{k}_m=\tfrac{k_m}{k_M},\ \bar{\alpha}_m=\tfrac{\alpha_m}{\alpha_M};\\ &\theta_{m,in}=\tfrac{T_{m,in}-T_{amb}}{T_{ref}-T_{amb}},\ Bi_A=\tfrac{h_A x_M}{k_M},\ Bi_B=\tfrac{h_B x_M}{k_M},\ Bi_m=\tfrac{h_m x_m}{k_m}\end{aligned} \tag{9}$$

The non-dimensional set of equations for the temperature field $\theta_m(\xi, \eta, \tau)$ is given by

$$\bar{\alpha}_m\left(\frac{\partial^2\theta_m}{\partial\xi^2}+\frac{\partial^2\theta_m}{\partial\eta^2}\right)=\frac{\partial\theta_m}{\partial\tau}(m=1,2..M) \tag{10}$$

$$-\bar{k}_1\frac{\partial\theta_1}{\partial\xi}+Bi_A\theta_1=0 \quad (\xi=0) \tag{11}$$

$$\frac{\partial\theta_M}{\partial\xi}+Bi_B\theta_M=0 \quad (\xi=1) \tag{12}$$

$$\frac{\partial\theta_m}{\partial\eta}=0 \quad (\eta=0) \tag{13}$$

$$\bar{k}_m\ \frac{\partial\theta_m}{\partial\eta}+Bi_m\theta_m=0 \quad (\eta=\bar{w}) \tag{14}$$

$$\theta_m=\theta_{m+1} \quad (\xi=\gamma_m)\ \ (m=1,2..M-1) \tag{15}$$

$$\bar{k}_m\frac{\partial\theta_m}{\partial\xi}=\bar{k}_{m+1}\frac{\partial\theta_{m+1}}{\partial\xi} \quad (\xi=\gamma_m)\ \ (m=1,2..M-1) \tag{16}$$

$$\theta_m=\theta_{m,in} \quad (\tau=0)(m=1,2..M) \tag{17}$$

2.3. Laplace transforms based solution technique

In order to derive an expression for the temperature field, a Laplace transformation of Eqs. (10)–(16) is first carried out. Using the initial condition given by Eq. (17), the governing equation for the Laplacian of the temperature field, $\hat{\theta}_m(\xi, \eta)$ is given by

$$\bar{\alpha}_m\left(\frac{\partial^2\hat{\theta}_m}{\partial\xi^2}+\frac{\partial^2\hat{\theta}_m}{\partial\eta^2}\right)=s\hat{\theta}_m-\theta_{m,in}(m=1,2..M-1) \tag{18}$$

where s is the Laplace variable.

The applicable boundary and interface conditions are

$$-\bar{k}_1\frac{\partial\hat{\theta}_1}{\partial\xi}+Bi_A\hat{\theta}_1=0 \quad (\xi=0) \tag{19}$$

$$\frac{\partial\hat{\theta}_M}{\partial\xi}+Bi_B\hat{\theta}_M=0 \quad (\xi=1) \tag{20}$$

$$\frac{\partial\hat{\theta}_m}{\partial\eta}=0 \quad (\eta=0)\ \ (m=1,2..M) \tag{21}$$

$$\bar{k}_m\ \frac{\partial\hat{\theta}_m}{\partial\eta}+Bi_m\hat{\theta}_m=0 \quad (\eta=\bar{w})\ \ (m=1,2..M) \tag{22}$$

$$\hat{\theta}_m=\hat{\theta}_{m+1} \quad (\xi=\gamma_m)\ \ (m=1,2..M-1) \tag{23}$$

$$\bar{k}_m\frac{\partial\hat{\theta}_m}{\partial\xi}=\bar{k}_{m+1}\frac{\partial\hat{\theta}_{m+1}}{\partial\xi}\ (\xi=\gamma_m)(m=1,2..M-1) \tag{24}$$

Solving Eq. (18)–(24) directly is difficult due to the inhomogeneity in Eq. (18) as well as the different Biot numbers along the wall in different layers. In order to proceed, the following transformation is first made:

$$\hat{\theta}_m=\hat{\varphi}_m(\xi,\eta)+\hat{u}_m(\eta) \tag{25}$$

By inserting Eq. (25) into Eq. (18), the $\hat{u}_m(\eta)$ problem may be defined by

$$\bar{\alpha}_m\frac{d^2\hat{u}_m}{d\eta^2}=s\hat{u}_m-\theta_{m,in} \qquad (m=1,2,3\ldots M) \tag{26}$$

Similarly, boundary conditions for $\hat{u}_m(\eta)$ may be defined as follows

$$\frac{d\hat{u}_m}{d\eta}=0 \quad (\eta=0)\ (m=1,2..M) \tag{27}$$

$$\bar{k}_m\frac{d\hat{u}_m}{d\eta}+Bi_m\hat{u}_m=0 \quad (\eta=\overline{w})(m=1,2..M) \tag{28}$$

A solution for $\hat{u}_m$ may be easily derived as follows:

$$\hat{u}_m(\eta)=C_m\cosh\left(\sqrt{\frac{s}{\bar{\alpha}_m}}\eta\right)+\frac{\theta_{m,in}}{s} \tag{29}$$

where

$$C_m = \frac{-Bi_m\theta_{m,in}/s}{\bar{k}_m\sqrt{\frac{s}{\bar{\alpha}_m}}\sinh\left(\sqrt{\frac{s}{\bar{\alpha}_m}}\bar{w}\right) + Bi_m\cosh\left(\sqrt{\frac{s}{\bar{\alpha}_m}}\bar{w}\right)} \quad (30)$$

The remainder of the problem, $\hat{\phi}_m(\xi,\eta)$ is then governed by

$$\bar{\alpha}_m\left(\frac{\partial^2\hat{\phi}_m}{\partial\xi^2} + \frac{\partial^2\hat{\phi}_m}{\partial\eta^2}\right) = s\hat{\phi}_m (m = 1, 2, 3 \ldots M) \quad (31)$$

subject to

$$-\bar{k}_1\frac{\partial\hat{\phi}_1}{\partial\xi} + Bi_A\hat{\phi}_1 = -Bi_A\hat{u}_1(\eta) \;\; (\xi = 0) \quad (32)$$

$$\frac{\partial\hat{\phi}_M}{\partial\xi} + Bi_B\hat{\phi}_M = -Bi_B\hat{u}_M(\eta) \quad (\xi = 1) \quad (33)$$

$$\frac{\partial\hat{\phi}_m}{\partial\eta} = 0 \quad (\eta = 0) \;\; (m = 1, 2..M) \quad (34)$$

$$\bar{k}_m \;\; \frac{\partial\hat{\phi}_m}{\partial\eta} + Bi_m\hat{\phi}_m = 0 \quad (\eta = \bar{w}) \;\; (m = 1, 2..M) \quad (35)$$

$$\hat{\phi}_m + \hat{u}_m(\eta) = \hat{\phi}_{m+1} + \hat{u}_{m+1}(\eta)(\xi = \gamma_m) \;\; (m = 1, 2..M-1) \quad (36)$$

$$\bar{k}_m\frac{\partial\hat{\phi}_m}{\partial\xi} = \bar{k}_{m+1}\frac{\partial\hat{\phi}_{m+1}}{\partial\xi} \quad (\xi = \gamma_m) \;\; (m = 1, 2..M-1) \quad (37)$$

The general solution for $\hat{\phi}_m$ is

$$\hat{\phi}_m(\xi,\eta) = \sum_{n=1}^{n=N}(A_{m,n}\cosh(\omega_{m,n}\xi) + B_{m,n}\sinh(\omega_{m,n}\xi))\cos(\lambda_{m,n}\eta)(m = 1, 2, 3 \ldots M) \quad (38)$$

Where $\omega_{m,n} = \sqrt{\lambda_{m,n}^2 + \frac{s}{\bar{\alpha}_m}}$.

Note that the sine term in the η direction is not considered in Eq. (38) due to the boundary condition at η=0, given by Eq. (34). Based on the boundary condition at $\eta = \bar{w}$ given by Eq. (35), the eigenvalues $\lambda_{m,n}$ for the m^{th} layer may be obtained as follows:

$$\bar{k}_m \;\; \lambda_{m,n}\sin(\lambda_{m,n}\bar{w}) - Bi_m\cos(\lambda_{m,n}\bar{w}) = 0 \quad (m = 1, 2..M) \quad (39)$$

Note that, in general, each layer has a unique set of eigenvalues.

Now, considering the first N terms of the series solution for $\hat{\phi}_m$, a total of $2\cdot N\cdot M$ coefficients ($A_{m,n}$ and $B_{m,n}$ with m=1,2..M and n=1,2..N) are unknown. In order to determine these coefficients and thus complete the solution, a set of $2\cdot N\cdot M$ linear algebraic equations are derived based on the boundary and interface conditions given by Eqs. (32), (33), (36), (37). This procedure is described next.

Inserting Eq. (38) in the boundary condition at ξ=0 given by Eq. (32) results in

$$\sum_{n=1}^{N}\left(-Bi_AA_{1,n} + \bar{k}_1\omega_{1,n}B_{1,n}\right)\cos(\lambda_{1,n}\eta) = Bi_A\hat{u}_1(\eta) \quad (40)$$

Multiplying Eq. (40) by $\cos(\lambda_{1,n'}\eta)$ and integrating from $\eta = 0$ to $\eta = \bar{w}$ results in

$$N_{1,n'}\left(-Bi_AA_{1,n'} + \bar{k}_1\omega_{1,n'}B_{1,n'}\right) = Bi_A\int_0^{\bar{w}}\cos(\lambda_{1,n'}\eta)\hat{u}_1(\eta)d\eta (n' = 1, 2, .., N) \quad (41)$$

Where $N_{m,n'} = \int_0^{\bar{w}}\cos^2(\lambda_{m,n'}\eta)d\eta$ is the norm for each layer. Similarly, inserting Eq. (38) in the boundary condition at ξ=1 given by Eq. (33), followed by multiplication by $\cos(\lambda_{M,n'}\eta)$ and integration from $\eta = 0$ to $\eta = \bar{w}$ results in

$$N_{M,n'}[(Bi_B\cosh(\omega_{M,n'}) + \omega_{M,n'}\sinh(\omega_{M,n'}))A_{M,n'} + (Bi_B\sinh(\omega_{M,n'}) + \omega_{M,n'}\cosh(\omega_{M,n'}))B_{M,n'}] = -Bi_B\int_0^{\bar{w}}\cos(\lambda_{M,n'}\eta)\hat{u}_M(\eta)d\eta \quad (42)$$

The heat flux and temperature conditions at each interface are utilized next. Inserting Eq. (38) into Eq. (37) for each m results in

$$\bar{k}_m\sum_{n=1}^{N}\omega_{m,n}(A_{m,n}\sinh(\omega_{m,n}\gamma_m) + B_{m,n}\cosh(\omega_{m,n}\gamma_m))\cos(\lambda_{m,n}\eta) = \bar{k}_{m+1}\sum_{n=1}^{N}\omega_{m+1,n}(A_{m+1,n}\sinh(\omega_{m+1,n}\gamma_m) + B_{m+1,n}\cosh(\omega_{m+1,n}\gamma_m))\cos(\lambda_{m+1,n}\eta) \quad (43)$$

Multiplying Eq. (43) by $\cos(\lambda_{m,n'}\eta)$ and integrating from $\eta = 0$ to $\eta = \bar{w}$ results in

$$\bar{k}_m\omega_{m,n'}(A_{m,n'}\sinh(\omega_{m,n'}\gamma_m) + B_{m,n'}\cosh(\omega_{m,n'}\gamma_m))N_{m,n'} = \bar{k}_{m+1}\sum_{n=1}^{N}\omega_{m+1,n}(A_{m+1,n}\sinh(\omega_{m+1,n}\gamma_m) + B_{m+1,n}\cosh(\omega_{m+1,n}\gamma_m))\int_0^{\bar{w}}\cos(\lambda_{m+1,n}\eta)\cos(\lambda_{m,n'}\eta)d\eta \quad (44)$$

Eq. (44) may be written for each $n' = 1, 2, ..N$ and for each interface $m = 1, 2, ..M-1$, and therefore represents a total of $N(M-1)$ equations.

Similarly to the procedure above, the temperature interface condition may be shown to result in the following set of equations as a result of multiplication by $\cos(\lambda_{m+1,n'}\eta)$ and integration from $\eta = 0$ to $\eta = \bar{w}$ along with the use of principle of orthogonality.

$$\sum_{n=1}^{N}(A_{m,n}\cosh(\omega_{m,n}\gamma_m) + B_{m,n}\sinh(\omega_{m,n}\gamma_m))\int_0^{\bar{w}}\cos(\lambda_{m,n}\eta)\cos(\lambda_{m+1,n'}\eta)d\eta = N_{m+1,n'}(A_{m+1,n'}\cosh(\omega_{m+1,n'}\gamma_m) + B_{m+1,n'}\sinh(\omega_{m+1,n'}\gamma_m)) + \int_0^{\bar{w}}\left(\hat{u}_{m+1}(\eta) - \hat{u}_m(\eta)\right)\cos(\lambda_{m+1,n'}\eta)d\eta \quad (45)$$

for $n' = 1, 2, ..N$ and $m = 1, 2, ..M-1$.

Together, Eqs. (41), (42), (44) and (45) represent $2\cdot N\cdot M$ equations each in an equal number of unknown coefficients $A_{m,n}$ and $B_{m,n}$. Therefore, this set of linear algebraic equations can be solved to determine these coefficients, which completes the solution of the problem in the Laplace domain.

Finally, inverse Laplace transformation of the solution, given by Eq. (25) may be carried out in order to determine the solution for $\theta(\xi,\eta,\tau)$. Due to the cumbersome nature of the solution in the Laplace domain, analytical inversion is not likely to be possible. Instead, several numerical algorithms for numerical inversion are available, such as Hollenbeck's algorithm [32], Talbot method [33] and the Carathéodory–Fejér method as used by Trefethen, et al. [34]. In the present work, Hollenbeck's algorithm is used. This algorithm has been used extensively for inverse Laplace transformation in past papers [6,35].

Even though the technique used here to solve the problem in the Laplace domain does not result in explicit expressions for all the coefficients in the infinite series, the approximation incurred is no worse than practical computation of the infinite series, for which also, only a finite number of terms can be practically computed. Similar to such computation, the accuracy of the present technique can be improved simply by considering a greater number of terms of the series solution.

3. Special Case – two-layer body

While the previous section derived the solution for a general M-layer problem, many practical problems involve only two layers. Moreover, much of past work on two-dimensional multilayer heat transfer considers only two-layer bodies [20–22]. Therefore, this section discusses the special case of a two-layer body, shown schematically in Fig. 1(b). An analytical solution for this case may be obtained from the general results of Section 2 by setting M=2. Further simplifications are also possible for this special case. It can be shown that the solution in Laplace domain is given by

$$\hat{\theta}_1(\xi,\eta) = C_1 \cosh\left(\sqrt{\frac{s}{\bar{\alpha}_1}}\eta\right) + \frac{\theta_{1,in}}{s} + \sum_{n=1}^{n=N}\left(A_{1,n}\cosh(\omega_{1,n}\xi) + B_{1,n}\sinh(\omega_{1,n}\xi)\right)\cos(\lambda_{1,n}\eta) \tag{46}$$

$$\hat{\theta}_2(\xi,\eta) = C_2 \cosh\left(\sqrt{s}\eta\right) + \frac{\theta_{2,in}}{s} + \sum_{n=1}^{n=N}\left(A_{2,n}\cosh(\omega_{2,n}(1-\xi)) + B_{2,n}\sinh(\omega_{2,n}(1-\xi))\right)\cos(\lambda_{2,n}\eta) \tag{47}$$

Where

$$C_1 = -\frac{Bi_1\theta_{1,in}}{s\left[\bar{k}_1\sqrt{\frac{s}{\bar{\alpha}_1}}\sinh\left(\sqrt{\frac{s}{\bar{\alpha}_1}}\bar{w}\right) + Bi_1\cosh\left(\sqrt{\frac{s}{\bar{\alpha}_1}}\bar{w}\right)\right]} \tag{48}$$

$$C_2 = -\frac{Bi_2\theta_{2,in}}{s\left[\sqrt{s}\sinh\left(\sqrt{s}\bar{w}\right) + Bi_2\cosh\left(\sqrt{s}\bar{w}\right)\right]} \tag{49}$$

Further, $B_{1,n}$ and $B_{2,n}$ are obtained from the solution of the following linear algebraic equations

$$\begin{aligned} &N_{1,n'}\bar{k}_1\omega_{1,n'}\left(\frac{-\sinh\left(\omega_{1,n'}\gamma_1\right)}{N_{1,n'}}\int_0^{\bar{w}}\hat{u}_1(\eta)\cos\left(\lambda_{1,n'}\eta\right)d\eta\right.\\ &\left.+B_{1,n'}\left[\cosh\left(\omega_{1,n'}\gamma_1\right) + \frac{\bar{k}_1\omega_{1,n'}}{Bi_A}\sinh\left(\omega_{1,n'}\gamma_1\right)\right]\right)\\ &= \sum_{n=1}^{N} -\omega_{2,n}\int_0^{\bar{w}}\cos(\lambda_{2,n}\eta)\cos\left(\lambda_{1,n'}\eta\right)d\eta\\ &\times\left(\frac{-\sinh(\omega_{2,n}(1-\gamma_1))}{N_{2,n}}\int_0^{\bar{w}}\hat{u}_2(\eta)\cos(\lambda_{2,n}\eta)d\eta\right.\\ &\left.+B_{2,n}\left[\cosh(\omega_{2,n}(1-\gamma_1)) + \frac{\omega_{2,n}}{Bi_B}\sinh\left(\omega_{2,n}(1-\gamma_1)\right)\right]\right) \end{aligned} \tag{50}$$

$$\begin{aligned} &\sum_{n=1}^{N}\int_0^{\bar{w}}\cos(\lambda_{1,n}\eta)\cos\left(\lambda_{2,n'}\eta\right)d\eta\left(\frac{-\cosh(\omega_{1,n}\gamma_1)}{N_{1,n}}\int_0^{\bar{w}}\hat{u}_1(\eta)\right.\\ &\left.\times\cos(\lambda_{1,n}\eta)d\eta + B_{1,n}\left[\sinh(\omega_{1,n}\gamma_1) + \frac{\bar{k}_1\omega_{1,n}}{Bi_A}\cosh(\omega_{1,n}\gamma_1)\right]\right)\\ &= N_{2,n'}\left(\frac{-\cosh\left(\omega_{2,n'}(1-\gamma_1)\right)}{N_{2,n'}}\int_0^{\bar{w}}\hat{u}_2(\eta)\cos\left(\lambda_{2,n'}\eta\right)d\eta\right.\\ &\left.+B_{2,n'}\left[\sinh\left(\omega_{2,n'}(1-\gamma_1)\right) + \frac{\omega_{2,n'}}{Bi_B}\cosh\left(\omega_{2,n'}(1-\gamma_1)\right)\right]\right)\\ &+\int_0^{\bar{w}}\cos\left(\lambda_{2,n'}\eta\right)\left(\hat{u}_2(\eta)-\hat{u}_1(\eta)\right)d\eta \end{aligned} \tag{51}$$

Finally, $A_{1,n}$ and $A_{2,n}$ are given by

$$A_{1,n} = \frac{\bar{k}_1\omega_{1,n}B_{1,n}}{Bi_A} - \frac{1}{N_{1,n}}\int_0^{\bar{w}}\hat{u}_1(\eta)\cos(\lambda_{1,n}\eta)d\eta \tag{52}$$

$$A_{2,n} = \frac{\omega_{2,n}B_{2,n}}{Bi_B} - \frac{1}{N_{2,n}}\int_0^{\bar{w}}\hat{u}_2(\eta)\cos(\lambda_{2,n}\eta)d\eta \tag{53}$$

Setting Bi_1 and Bi_2 to infinity reduces the general solution derived here to the one for isothermal conditions derived in past work.

4. Results and discussion

4.1. Number of terms needed in series solution

It is important to carry out convergence analysis for an infinite series based solution, such as the one derived in this work. In particular, it is critical to determine the minimum number of terms, N, needed to be included in the system of linear equations Eqs. (41), ((42), (44) and (45)) in order to appropriately balance computational time and accuracy. Towards this, a representative two-layer problem is solved with different values of N while all other parameters are held constant. The problem parameters used for this analysis are $Bi_A = 2$, $Bi_B = 4$, $Bi_1 = 1$, $Bi_2 = 10$ $\gamma_1 = 0.5$, $\bar{w} = 2$, $\bar{k}_1 = 4$, $\bar{\alpha}_1 = 1.8$. The initial temperature is assumed to be 1 throughout each layer in this and all subsequent analysis presented in this work. Results are presented in Fig. 2, in which temperature distributions in the ξ and η directions at $\tau = 1$ are plotted for different values of N in Fig. 2(a) and 2(b), respectively. Temperature in the ξ direction is plotted at $\eta = 1$, whereas temperature in the η direction is plotted at $\xi = 0.75$. Results indicate convergence of predicted temperature distribution as N increases. In particular, the predicted temperature distribution in both directions remains practically the same between N=30 and N=40. Therefore, all calculations in this work are carried out with 30 terms in the series solution. Note that there is minimal increase in computational cost between N=30 and N=40 because even a linear system of 40 equations is relatively straightforward to compute. Therefore, in general, in this case, it is recommended to include a large number of terms in order to improve accuracy without significant penalty in terms of computational cost.

Note that a rigorous mathematical convergence analysis for this problem is not possible because the coefficients for various terms are expressed in terms of the solution of a system of linear equations. Nevertheless, the analysis described above helps estimate the number of terms needed for reasonable accuracy in the range of parameters considered here. For other problems in which the values of these parameters may be very different than ones considered here, it is recommended to carry out an analysis similar to one described above. Moreover, given the small incremental penalty of computational cost, it is recommended not to be conservative about the number of terms considered in calculations.

4.2. Comparison with numerical simulations

In order to further establish the accuracy of the theoretical technique used in this work, results from the present work are compared against fully numerical simulations for the problem based on finite-element analysis. For a representative set of parameters ($Bi_A = 2$, $Bi_B = 4$, $\gamma_1 = 0.5$, $\bar{w} = 2$, $\bar{k}_1 = 4$, $\bar{\alpha}_1 = 1.8$), Fig. 3(a) plots temperature distributions in the η direction at $\xi = 0.25$ at multiple times. Fig. 3(b) plots the variation of temperature over time at the centers of the two layers. Curves based on the present work and numerical simulations are both presented for comparison. Note that both layers have a general convective boundary condition, with $Bi_1 = 1$ and $Bi_2 = 10$ for the wall normal to the layered

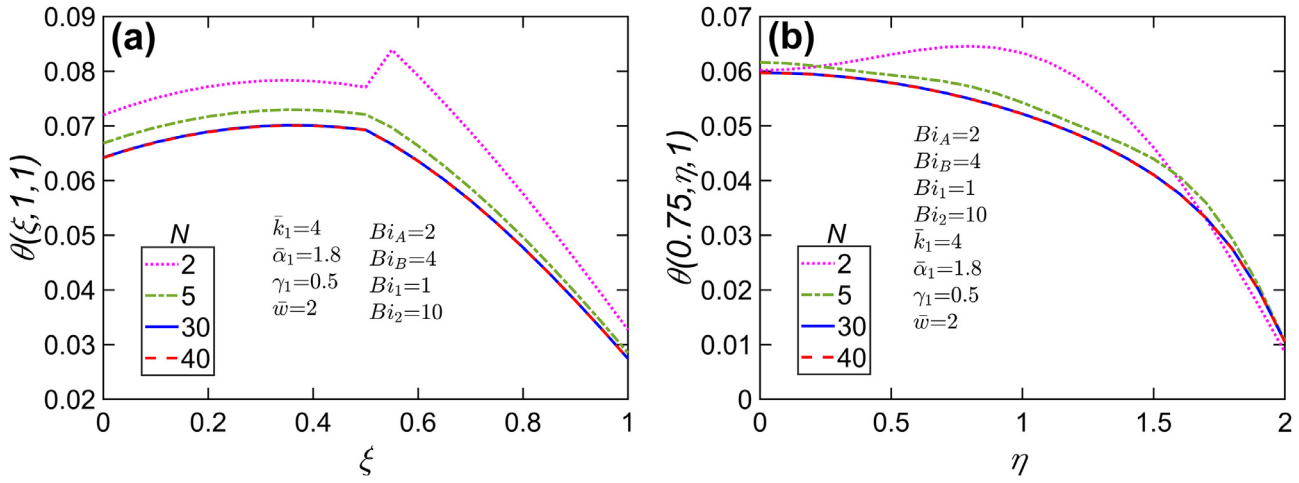

Fig. 2. Effect of number of eigenvalues: (a) θ vs ξ at $\eta = \bar{w}/2$ and τ =1, (b) θ vs η at ξ =0.75 and τ =1. Problem parameters are $\bar{\alpha}_1$=1.8, $\bar{k}_1$=4, γ_1=0.5, $\bar{w}$=2, Bi_1=1, Bi_2=10, Bi_A=2 and Bi_B=4.

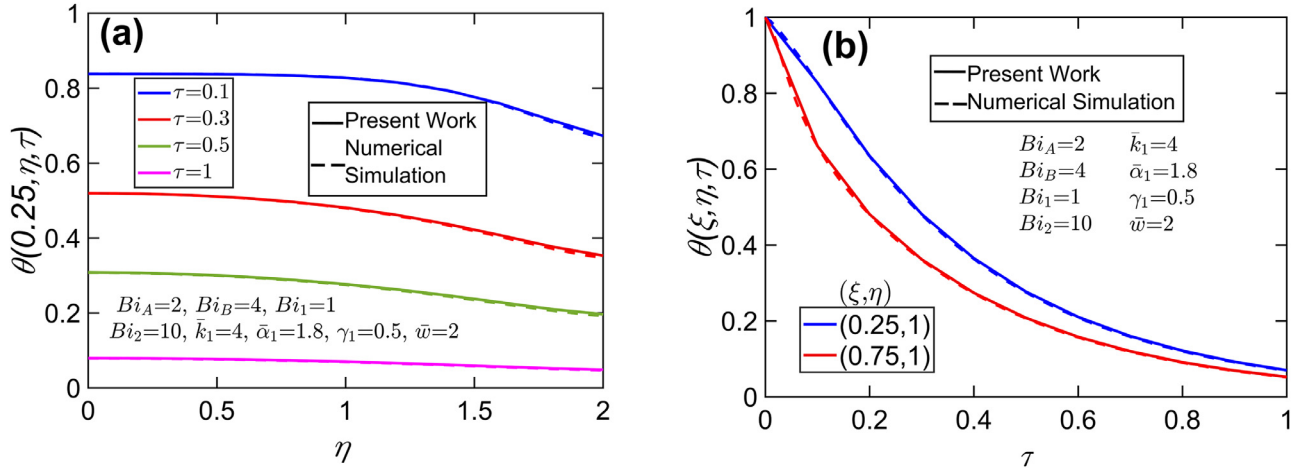

Fig. 3. Comparison of present work with numerical simulations: (a) θ vs η at ξ =0.25 for multiple times, (b) θ vs τ at the center of layers 1 and 2. Problem parameters are $\bar{\alpha}_1$=1.8, $\bar{k}_1$=4, γ_1=0.5, $\bar{w}$=2, Bi_1=1, Bi_2=10, Bi_A=2 and Bi_B=4.

direction. Fig. 3 shows excellent agreement between the present work and numerical simulations, both in terms of spatial and temporal distributions. The worst-case deviation between the two is found to be less than 1%. As expected, the temperature distribution decays over time, and the solution based on the theoretical technique is able to correctly capture the nature of the temperature solution over time and in space.

Note that the total computation time for calculating the temperature at one specific location and time using the theoretical technique is estimated to be around 2.5 s, compared to 20.0 s for the finite-element numerical simulations discussed above. This comparison is even more favorable for the theoretical technique at large times, since numerical simulations typically need to march throughout the entire duration prior to the time of interest. Further, the theoretical technique does not require time for geometrical modeling or mesh generation, and provides a more comprehensive fundamental understanding of the problem. On the other hand, the theoretical technique is limited in its capability to handle complicated geometry and secondary effects such as temperature-dependent properties, which numerical techniques are usually better at. Regardless, it is to be noted that the goal of the present work is to develop a novel theoretical technique rather than to compete with numerical methods.

4.3. Comparison with past work

The theoretical model discussed in Section 2 represents a generalization of past work, in that general convective boundary conditions are considered in the η direction, whereas past work is only able to account for the limiting cases of isothermal and adiabatic boundary conditions. Therefore, it is instructive to compare the results from the present work with past papers for special cases of isothermal and adiabatic boundary conditions in the η direction.

Two special cases are considered for comparison with past work. Firstly, for very small values of Bi_1 and Bi_2, thermal conduction in the two-layer geometry is expected to become purely one-dimensional in the ξ direction, since the initial temperature distribution is also independent of η. In such a case, the problem reduces to a one-dimensional multilayer diffusion problem, for which, standard analytical solutions based on multilayer quasi-orthogonality of eigenfunctions is available [11,16]. Therefore, a comparison of the present work with a one-dimensional multilayer problem is carried out. For a representative problem with $Bi_A = 2$, $Bi_B = 2$, $\gamma_1 = 0.5$, $\bar{w} = 2$, $\bar{k}_1 = 4$, $\bar{\alpha}_1 = 1.8$, Fig. 4 plots the temperature distribution as a function of ξ at $\tau = 0.3$ for multiple values of the Biot number at $\eta = \bar{w}/2$, assumed to be the same for both layers. For comparison, the temperature distribution predicted for a

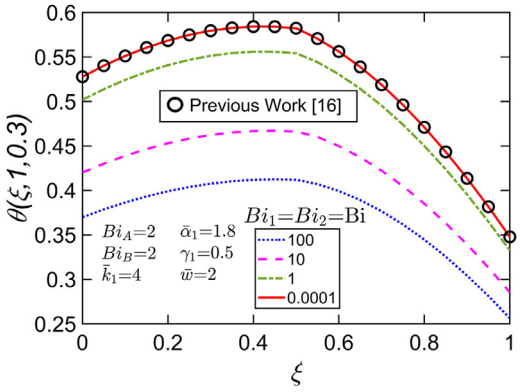

Fig. 4. Comparison of present work with past work [16]: θ vs ξ at $\eta = \bar{w}/2$ and τ =0.3 for multiple values of η direction Biot number (Bi_1=Bi_2). Problem parameters are $\bar{\alpha}_1$=1.8, $\bar{k}_1$=4, γ_1=0.5, $\bar{w}$=2, Bi_A=2 and Bi_B=2.

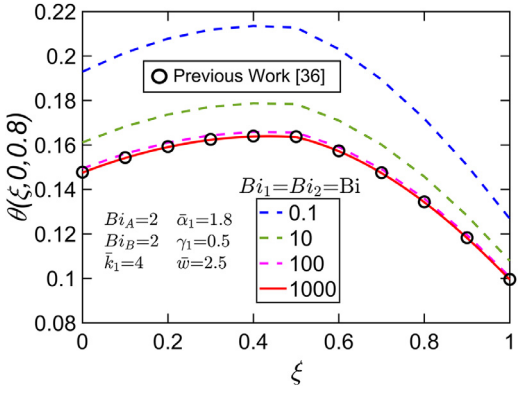

Fig. 5. Comparison of present work with past work [36]: θ vs ξ at η =0 and τ=0.8 for multiple values of η direction Biot number (Bi_1=Bi_2). Problem parameters are $\bar{\alpha}_1$=1.8, $\bar{k}_1$=4, γ_1=0.5, $\bar{w}$=2.5, Bi_A=2 and Bi_B=2.

one-dimensional multilayer problem [16] with the same set of parameter values is also plotted. As the value of the Biot number at $\eta = \bar{w}$ decreases, Fig. 4 shows that the temperature distribution for the 2D multilayer problem approaches that for a one-dimensional multilayer problem. At a value of 0.0001 for the Biot number, the two curves are practically identical. This shows that the 2D multilayer problem solved in this work correctly reduces to a 1D multilayer form for the special case of small Biot number in the η direction.

A second comparison with past work is carried out for the special case where the Biot number in the η direction becomes very large. In this case, the general convective problem considered in this work reduces to one in which the boundaries are isothermal. This problem has been recently solved for a two-dimensional multilayer geometry [36]. A comparison between the present work and this past work is carried out for this special case. Problem parameter values are taken to be $Bi_A = 2$, $Bi_B = 2$, $\gamma_1 = 0.5$, $\bar{w} = 2.5$, $\bar{k}_1 = 4$, $\bar{\alpha}_1 = 1.8$ along with an initial condition of 1 throughout the body. Fig. 5 presents this comparison in terms of temperature distribution as a function of ξ for multiple values of the Biot number in the η direction at $\tau = 0.8$ and $\eta = 0$. As expected, results from the present work get closer and closer to the isothermal result from past work as the value of the Biot number increases. For $Bi = 1000$, the two curves practically coincide.

The good agreement between the present work and past theoretical models for special cases of small and large values of the Biot number as shown in Figs. 4 and 5 is encouraging.

Further, a comparison of the present work is carried out with work by de Monte [22] that addressed the two-dimensional two-

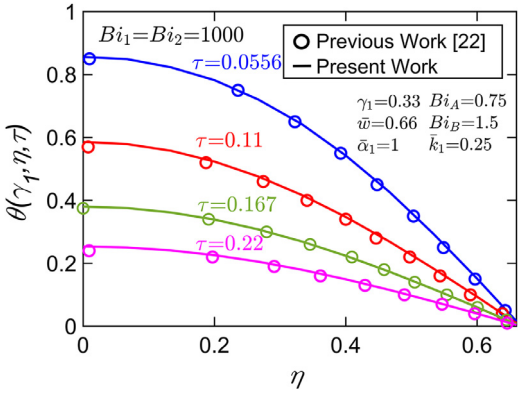

Fig. 6. Comparison of present work with past work [22]: θ vs η at ξ=γ_1 for multiple times. Problem parameters are $\bar{\alpha}_1$=1, $\bar{k}_1$=0.25, γ_1=0.33, $\bar{w}$=0.66, Bi_1=1000, Bi_2=1000, Bi_A=0.75 and Bi_B=1.5.

layer diffusion problem only for the special case of isothermal or adiabatic boundary conditions in the η direction. This past paper utilized a separation of variables approach for this transient problem, due to which, the analysis was limited only to adiabatic or isothermal boundary conditions, and, in addition, the two layers were also assumed to have the same thermal diffusivity. While the present analysis is a lot more general, allowing for general convective boundary conditions, as well as unequal thermal diffusivities of the layers, it is instructive to compare the present work with de Monte [22] for a special case that satisfies the restrictions of the past work. In order to do so, calculations based on the present work are carried out for the parameter values specified in the numerical results presented by de Monte. These non-dimensional parameters are carefully transformed to the non-dimensional scheme used in the present work. The transformed parameters used for comparison are $Bi_A = 0.75$, $Bi_B = 1.5$, $\gamma_1 = 0.33$, $\bar{w} = 0.66$, $\bar{k}_1 = 0.25$, $\bar{\alpha}_1 = 1$. Note that the values of the non-dimensional time are different between de Monte and the present work due to differences in the non-dimensionalization scheme. Fig. 6 presents a comparison between the present work and de Monte [22] in terms of interfacial temperature distribution in the η direction at multiple times, starting with a uniform initial temperature. Note that the values of non-dimensional time shown in Fig. 6 correspond to the non-dimensionalization scheme followed in the present work. Fig. 6 shows excellent agreement between the two at each time considered and demonstrates that the present work correctly reduces to de Monte's results for the special case that the past work is valid for. By allowing for a general convective boundary condition and unequal thermal diffusivities, the present work is a lot more general than de Monte [22] and encompasses a much broader set of two-dimensional multilayer problems.

4.4. Typical temperature colorplots

Based on the solution technique described in previous sections, a representative two-layer problem is solved. The problem parameters are $\bar{\alpha}_1$=1.8, $\bar{k}_1$=4, γ_1=0.5, $\bar{w}$=2.5, Bi_1=1, Bi_2=10, Bi_A=2 and Bi_B=4. Fig. 7 presents colorplots of the temperature distribution in the entire body at multiple times, starting with a uniform initial temperature of one. As expected, the temperature field decays over time, faster in layer 1, due to greater thermal conductivity and diffusivity of layer 1 and despite the smaller Biot number at the $\xi = 0$ end than at the $\xi = 1$ end. Within each layer, the temperature field close to the convective boundaries is lower than away from it, particularly near the adiabatic boundary, which is also along expected lines. As time increases, the temperature field, in general, decays due to heat removal from the convective boundaries. The impact

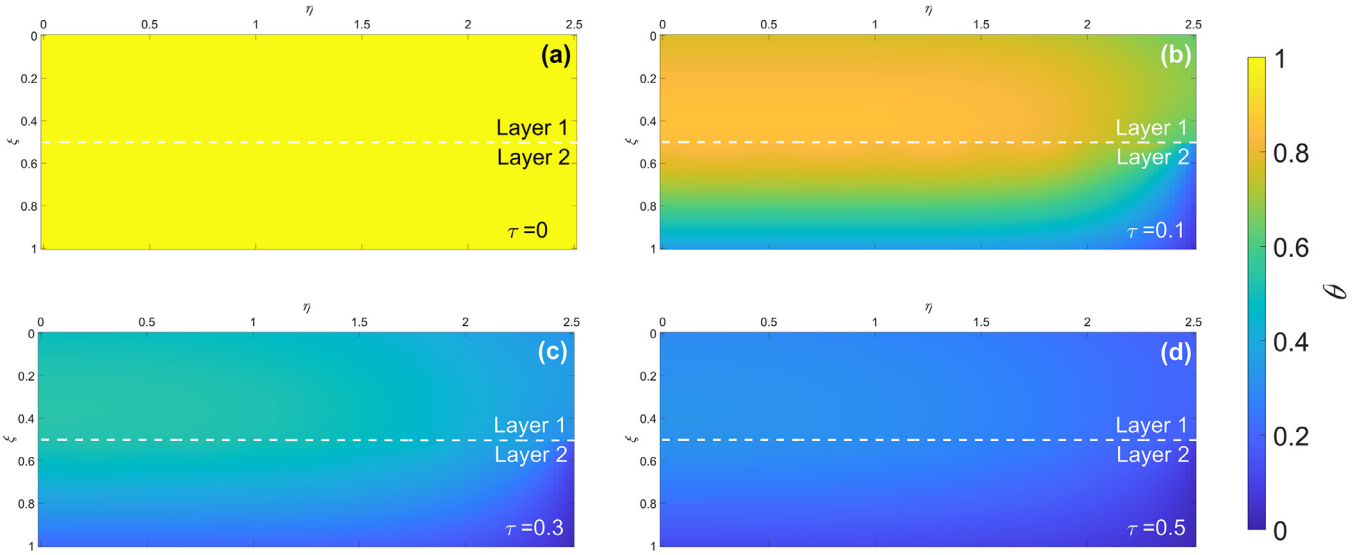

Fig. 7. Temperature contours for a representative two-layer problem at (a) τ=0, (b) τ=0.1, (c) τ=0.3, (d) τ=0.5. Problem parameters are $\bar{\alpha}_1$=1.8, $\bar{k}_1$=4, γ_1=0.5, $\bar{w}$=2.5, Bi_1=1, Bi_2=10, Bi_A=2 and Bi_B=4.

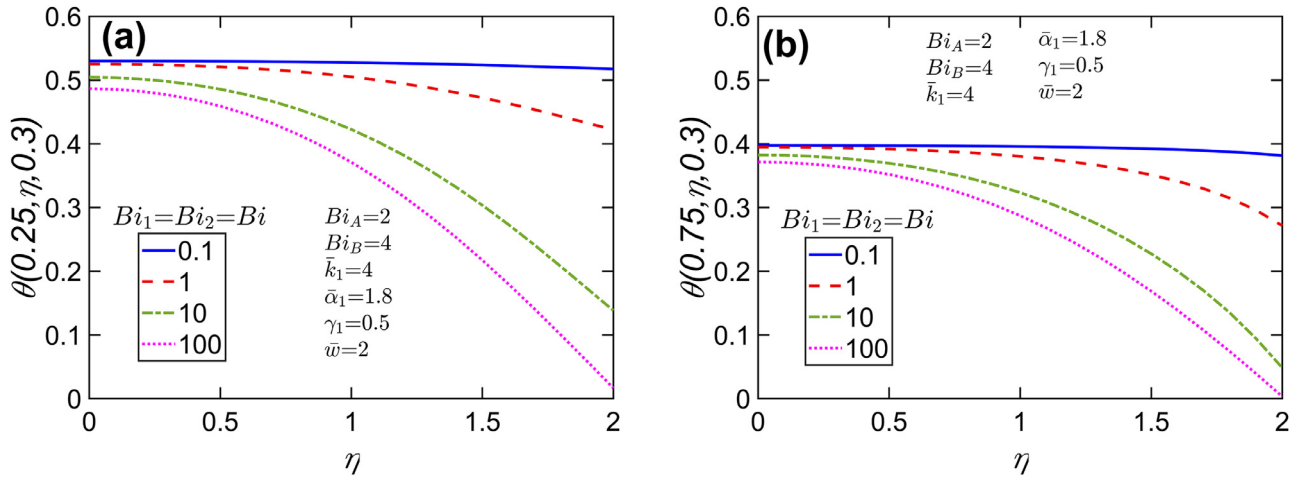

Fig. 8. Impact of η direction Biot number: (a) θ vs η at $\xi = 0.25$ and τ =0.3, (b) θ vs η at $\xi = 0.75$ and τ =0.3. Problem parameters are $\bar{\alpha}_1$=1.8, $\bar{k}_1$=4, γ_1=0.5, $\bar{w}$=2, Bi_1=1, Bi_2=10, Bi_A=2 and Bi_B=4.

of key parameters, such as the Biot numbers and the ratio of diffusivities is presented in the next sub-sections.

4.5. Impact of Biot number in η direction on temperature distribution

In addition to verification, Figs. 4 and 5 also illustrate interesting features of thermal conduction in a 2D multilayer geometry, particularly the impact of the Biot number in the η direction. For example, both Figures show a reduction in the temperature distribution as the Biot number in the η direction increases, which is consistent with more effective heat removal at large values of the Biot number. Further investigation of the impact of the Biot number in the η direction on temperature distribution is presented in subsequent Figures.

The effect of the Biot number in the η direction on temperature distribution along the η direction at $\tau = 0.3$ is presented in Fig. 8. The Biot numbers at $\xi = 0$ and $\xi = 1$ are $Bi_A = 2$ and $Bi_B = 4$, respectively. All the other problem parameter values are the same as Fig. 4. Fig. 8(a) and 8(b) present plots along the middle of layers 1 and 2, respectively. These plots, as expected, show spatial variation of temperature in the η direction as the value of Biot number along the $\eta = \bar{w}$ boundary increases. In contrast, the temperature distribution is quite flat when the Biot number is relatively small. This is because of significant heat removal from the $\eta = \bar{w}$ boundary at large Biot numbers, whereas, when the Biot number is small, there is no heat loss from this boundary, resulting in heat flow only along the ξ direction, and, therefore, a largely one-dimensional temperature distribution. In addition, these plots also show, as expected, lower temperature with increasing value of Biot number, due to improved heat removal from the boundaries. Finally, as the Biot number in the η direction becomes larger and larger, the temperature at the $\eta = \bar{w}$ boundary is seen to become closer and closer to zero, which is consistent with the boundary approaching isothermal conditions for large values of the Biot number. In contrast, as the Biot number reduces, the curves in Fig. 8(a) and 8(b) are found to become flatter and flatter, indicating that the temperature distribution becomes more and more one-dimensional, i.e., independent of η.

The evolution of the temperature field over time is illustrated in Fig. 9(a), which plots temperature at a fixed location as a function of time for the same parameter values as Fig. 8. As expected, this plot shows that the temperature at a point reduces over time, rapidly at first and then slower at larger time, eventually decaying to zero. This illustrates the eventual loss of all of the initial ther-

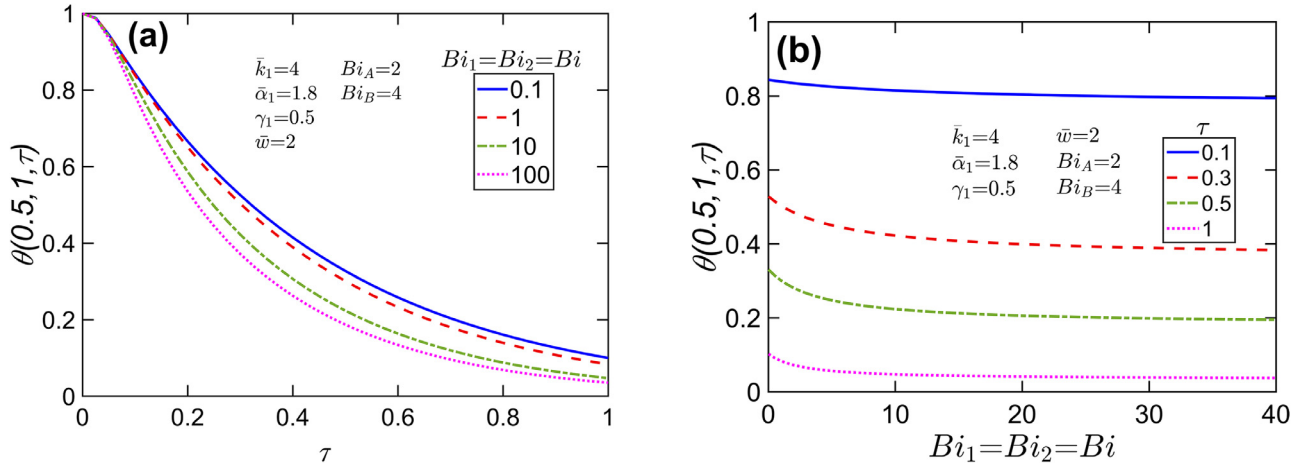

Fig. 9. Special cases showing the effect of η direction Biot number (Bi_1=Bi_2=Bi): (a) θ vs τ at the center for multiple values of Bi, (b) θ vs Bi at the center for multiple times. Problem parameters are $\tilde{\alpha}_1$=1.8, $\bar{k}_1$=4, γ_1=0.5, $\bar{w}$=2, Bi_A=2 and Bi_B=4.

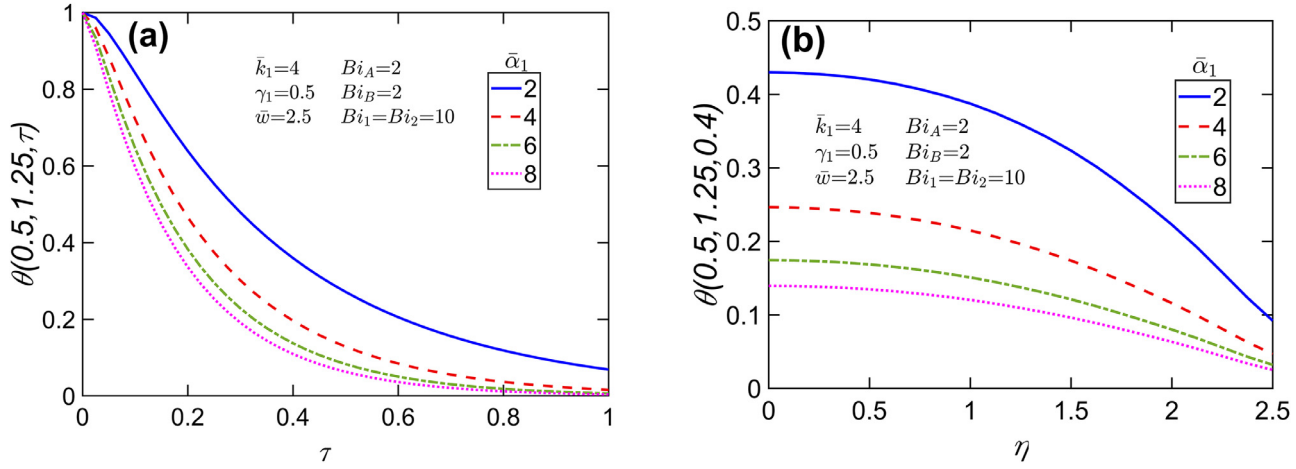

Fig. 10. Effect of thermal diffusivity: (a) θ vs τ at the center of the geometry for multiple values of $\tilde{\alpha}_1$, (b) θ vs η at $\xi = 0.5$ and τ =0.4 for multiple values of $\tilde{\alpha}_1$. Parameters for this two-layer problem are $\bar{k}_1$=4, γ_1=0.5, $\bar{w}$=2.5, Bi_1=10, Bi_2=10, Bi_A=2 and Bi_B=2.

mal energy in the two-layer body from the convective boundaries in the ξ and η directions. Further, Fig. 9(a) shows greater rate of reduction of temperature at larger values of the Biot number in the η direction due to stronger convective heat removal from the boundaries, although this is not a strong influence at small times, when conduction to the boundary is not well established, or at large times, when most of the heat has already conducted away from the body.

Fig. 9(b) presents the impact of the Biot number in the η direction on temperature at the same location as Fig. 9(a). As expected, for a given time, as the Biot number increases, the temperature reduces due to the boundary permitting more and more heat removal. For a sufficiently large value of the Biot number, however, the boundary is sufficiently close to isothermal, and, therefore, there is no significant further reduction in temperature with further increase in the Biot number. Fig. 9(b) also illustrates the decay in the temperature field over time. Curves plotted at increasing values of time show lower and lower temperature.

4.6. Impact of thermal diffusivity

Finally, the effect of thermal diffusivity on the temperature distribution is analyzed. For a representative problem, temperature at the center of the two-layer body is plotted as a function of time for multiple values of $\tilde{\alpha}_1$ in Fig. 10(a). The associated problem parameters are $Bi_1 = 10, Bi_2 = 10, Bi_A = 2, Bi_B = 2, \gamma_1 = 0.5, \bar{w} = 2.5, \bar{k}_1 = 4$. As expected, increasing $\tilde{\alpha}_1$ results in greater heat dissipation from the first layer to the heat-removing boundaries, and, therefore, reduction in temperature and the rate of thermal decay. The spatial variation of interface temperature in the η direction at $\tau = 0.4$ is plotted in Fig. 10(b). Consistent with Fig. 10(a), as the value of $\tilde{\alpha}_1$ increases, Fig. 10(b) shows reduced temperature. Fig. 10(b) also shows greater thermal uniformity within the body at large values of $\tilde{\alpha}_1$, which is consistent with greater ability to diffuse heat within the first layer.

5. Conclusions

The transient multilayer two-dimensional diffusion problem has been solved in the past only for the special case of isothermal or adiabatic conditions normal to the layered direction. The key contribution of this work is in generalizing this to include general convective boundary conditions instead. While presented in the context of a heat transfer problem, the technique is also applicable for equivalent mass transfer problems. Further, the pure diffusion analysis presented in this work can be easily extended to multilayer two-dimensional diffusion-reaction problems by appropriately accounting for the reaction coefficient in the definition of the eigenvalues, as has been done for one-dimensional diffusion-reaction problems [15,16,19]. Extension to three-dimensional prob-

lems is also fairly straightforward, as this will only involve one new set of eigenvalues. Finally, note that the derivation in this work explicitly assumes uniform initial temperature in each layer, which is a reasonable assumption for a wide variety of problems. Extension to account for non-uniformity, such as in the η direction is cumbersome, but possible. Depending on the specific nature of such non-uniformity, this may require deriving a new solution for Eq. (26), since Eq. (29) in the present work is specific to a uniform initial temperature. The rest of the methodology is expected to remain unaffected.

The analytical technique discussed here improves the fundamental understanding of multilayer diffusion problems. In addition, the capability to analyze two-dimensional multilayer diffusion with general convective boundary conditions may be pertinent to several practical engineering problems.

Declaration of Competing Interest

The authors declare that they have no known competing financial interests or personal relationships that could have appeared to influence the work reported in this paper.

CRediT authorship contribution statement

Girish Krishnan: Methodology, Formal analysis, Investigation, Data curation, Visualization, Writing – original draft, Writing – review & editing. **Ankur Jain:** Conceptualization, Formal analysis, Methodology, Supervision, Project administration, Data curation, Visualization, Writing – original draft, Writing – review & editing.

Data Availability

Data will be made available on request.

Acknowledgment

This material is based upon work supported by CAREER Award No. CBET-1554183 from the National Science Foundation.

References

[1] K. Shah, V. Vishwakarma, A. Jain, Measurement of multiscale thermal transport phenomena in Li-ion cells: a review, J. Electrochem. Energy Convers. Storage 13 (2016), doi:10.1115/1.4034413.
[2] L. Choobineh, A. Jain, An explicit analytical model for rapid computation of temperature field in a three-dimensional integrated circuit (3D IC), Int. J. Therm. Sci. 87 (2015) 103–109, doi:10.1016/j.ijthermalsci.2014.08.012.
[3] K. Daryabeigi, Thermal analysis and design of multi-layer insulation for Re-entry aerodynamic heating, J. Spacecr. Rockets 39 (2002) 509–514, doi:10.2514/2.3863.
[4] S.M. Becker, H. Herwig, One dimensional transient heat conduction in segmented fin-like geometries with distinct discrete peripheral convection, Int. J. Therm. Sci. 71 (2013) 148–162, doi:10.1016/j.ijthermalsci.2013.04.004.
[5] H. French, Heat Transfer and Fluid Flow in Nuclear Systems, 1st Ed., Pergamon Press, 1981 ISBN: 978-1483118369.
[6] G. Krishnan, M. Parhizi, M. Pathak, A. Jain, Solution phase limited diffusion modeling in a Li-ion cell subject to concentration-dependent pore wall flux, J. Electrochem. Soc. 168 (2021) 090511, doi:10.1149/1945-7111/ac1cfb.
[7] V.R. Subramanian, D. Tapriyal, R.E. White, A boundary condition for porous electrodes, Electrochem. Solid State Lett. 7 (2004), doi:10.1149/1.1773751.
[8] A. Jain, S. McGinty, G. Pontrelli, L. Zhou, Theoretical modeling of endovascular drug delivery into a multilayer arterial wall from a drug-coated balloon, Int. J. Heat Mass Trans. 187 (2022) 122572, doi:10.1016/j.ijheatmasstransfer.2022.122572.
[9] H.S. Carslaw, J.C. Jaeger, Conduction of Heat in Solids, Clarendon Press, Oxford, 1959.
[10] T.R. Goodman., The Adjoint Heat-Conduction Problems for Solids, ASTIA-AD 254–769, (AFOSR-520), April 1961.
[11] D.W. Hahn, M.N. Özışık, Heat Conduction, 3rd ed, Wiley, Hoboken, N.J., 2012.
[12] C.W. Tittle, Boundary value problems in composite media: quasi-orthogonal functions, J. Appl. Phys. 36 (1965) 1486–1488, doi:10.1063/1.1714335.
[13] L. Zhou, M. Parhizi, A. Jain, Theoretical modeling of heat transfer in a multilayer rectangular body with spatially-varying convective heat transfer boundary condition, Int. J. Therm. Sci. 170 (2021) 107156, doi:10.1016/j.ijthermalsci.2021.107156.
[14] R. Chiba, An analytical solution for transient heat conduction in a composite slab with time-dependent heat transfer coefficient, Math. Probl. Eng. 2018 (2018), doi:10.1155/2018/4707860.
[15] A. Jain, L. Zhou, M. Parhizi, Multilayer one-dimensional Convection-Diffusion-Reaction (CDR) problem: analytical solution and imaginary eigenvalue analysis, Int. J. Heat Mass Trans. 177 (2021), doi:10.1016/j.ijheatmasstransfer.2021.121465.
[16] A. Jain, M. Parhizi, L. Zhou, G. Krishnan, Imaginary eigenvalues in multilayer one-dimensional thermal conduction problem with linear temperature-dependent heat generation, Int. J. Heat Mass Trans. 170 (2021), doi:10.1016/j.ijheatmasstransfer.2021.120993.
[17] E.J. Carr, Generalized semi-analytical solution for coupled multispecies advection-dispersion equations in multilayer porous media, Appl. Math. Modell. 94 (2021) 87–97, doi:10.1016/j.apm.2021.01.013.
[18] E.J. Carr, I.W. Turner, A semi-analytical solution for multilayer diffusion in a composite medium consisting of a large number of layers, Appl. Math. Modell. 40 (2016) 7034–7050, doi:10.1016/j.apm.2016.02.041.
[19] G. Krishnan, A. Jain, Derivation of multiple but finite number of imaginary eigenvalues for a two-layer diffusion-reaction problem, Int. J. Heat Mass Trans. 194 (2022), doi:10.1016/j.ijheatmasstransfer.2022.123037.
[20] A. Haji-Sheikh, J. Beck, D. Agonafer, Steady-state heat conduction in multilayer bodies, Int. J. Heat Mass Trans. 46 (2003) 2363–2379, doi:10.1016/S0017-9310(02)00542-2.
[21] A. Haji-Sheikh, J. Beck, Temperature solution in multi-dimensional multilayer bodies, Int. J. Heat Mass Trans. 45 (2002) 1865–1877, doi:10.1016/S0017-9310(01)00279-4.
[22] F. de Monte, Unsteady heat conduction in two-dimensional two slab-shaped regions. Exact closed-form solution and results, Int. J. Heat Mass Trans. 46 (2003) 1455–1469, doi:10.1016/S0017-9310(02)00417-9.
[23] H. Salt, Transient conduction in a two-dimensional composite slab—II. Physical interpretation of temperature modes, Int. J. Heat Mass Trans. 26 (1983) 1617–1623, doi:10.1016/S0017-9310(83)80081-7.
[24] M.D. Mikhailov, M.N. Özişik, Transient conduction in a three-dimensional composite slab, Int. J. Heat Mass Trans. 29 (1986) 340–342, doi:10.1016/0017-9310(86)90242-5.
[25] H. Levine, Unsteady diffusion in a composite medium, Quart. J. Mech. Appl. Math. 52 (4) (1999) 499–512, doi:10.1093/qjmam/52.4.499.
[26] V.P. Kozlov, P.A. Mandrix, Method of summation-integral equations for solving the mixed problem of non stationary heat conduction, J. Eng. Phys. Thermophys. 74 (2) (2001) 477–486, doi:10.1023/A:1016637413073.
[27] V.P. Kozlov, P.A. Mandrix, Solution of mixed contact problems in the theory of nonstationary heat conduction by the method of summation-integral equations, J. Eng. Phys. Thermophys. 74 (3) (2001) 632–637, doi:10.1023/A:1016752126279.
[28] S.W. Ma, A.I. Behbahani, Y.G. Tsuei, Two-dimensional rectangular fin with variable heat transfer coefficient, Int. J. Heat Mass Trans. 34 (1991) 79–85, doi:10.1016/0017-9310(91)90175-E.
[29] D. Sarkar, K. Shah, A. Haji-Sheikh, A. Jain, Analytical modeling of temperature distribution in an anisotropic cylinder with circumferentially-varying convective heat transfer, Int. J. Heat Mass Trans. 79 (2014) 1027–1033, doi:10.1016/j.ijheatmasstransfer.2014.08.060.
[30] G. Krishnan, A. Jain, Theoretical heat transfer analysis of a multi-layered semiconductor device with spatially-varying thermal contact resistance between layers, Int. Commun. Heat Mass Trans. 140 (2023) 106482, doi:10.1016/j.icheatmasstransfer.2022.106482.
[31] N.G. March, E.J. Carr, I.W. Turner, A fast algorithm for semi-analytically solving the homogenization boundary value problem for block locally-isotropic heterogeneous media, Appl. Math. Modell. 92 (2021) 23–43, doi:10.1016/j.apm.2020.09.022.
[32] K.J. Hollenbeck, INVLAP.M: A Matlab Function for Numerical Inversion of Laplace Transforms by the de Hoog Algorithm, 1998 available at http://www.isva.dtu.dk/staff/karl/invlap.htm accessed 1/1/2012.
[33] A. Talbot, The accurate numerical inversion of Laplace transforms, IMA J. Appl. Math. 23 (1979) 97–120, doi:10.1093/imamat/23.1.97.
[34] L.N. Trefethen, J.A.C. Weideman, T. Schmelzer, Talbot quadratures and rational approximations, BIT Numer. Math. 46 (2006) 653–670, doi:10.1007/s10543-006-0077-9.
[35] L. Choobineh, A. Jain, Analytical solution for steady-state and transient temperature fields in vertically stacked 3-D integrated circuits, IEEE Trans. Compon. Packag. Manuf. Technol. 2 (2012) 2031–2039, doi:10.1109/TCPMT.2012.2213820.
[36] G. Krishnan, A. Jain, Diffusion and reaction in a two-dimensional multilayer body: analytical solution and imaginary eigenvalue analysis, Int. J. Heat Mass Trans. 196 (2022) 123163, doi:10.1016/j.ijheatmasstransfer.2022.123163.